Investigation of the porosity influence on dynamic tensile strength of polycrystalline ice

D. GEORGES[a,b], D. SALETTI[a], M.MONTAGNAT[b], P.FORQUIN[a]

a. Univ. Grenoble Alpes, CNRS, Grenoble INP 1 , 3SR, F-38000 Grenoble, France
b. Univ. Grenoble Alpes, CNRS, Grenoble INP 1 , IGE, F-38000 Grenoble, France

Abstract :

Polycrystalline ice has been extensively investigated during the last decades regarding its mechanical behaviour for quasi-static loadings. Conversely, only few studies can be found on its dynamic behaviour and scientists suffer from a lack of experimental observation to develop relevant modelling at high strain rate ranges. Dynamic experiments have already been conducted in compression mode using Hopkinson bar set-up. Regarding tension, the literature gives only approximated strength values and experimental observations and measurements are scarce. This knowledge is essential to design structures that may experience ice impact. The present study aims at providing complementary results to the first reproducible experimental data of the tensile strength of polycrystalline ice subjected to dynamic tensile loading presented in Salettie et al. [12]. In addition to this previous work a particular focus has been made on porosity influence. To do so, a spalling test technique has been used on two differenct ice microstructures with a different porosity, to apply tensile loading at strain rates from $24\ s^{-1}$ *to* $120\ s^{-1}$ *. The experimental results show that the tensile strength is sensitive to the applied strain rate, and seems to be weakened by an increase of the porosity.*

Mots clefs : ice, spalling test, dynamic tensile strength, microstructure effect, strain rate sensitivity

1 Introduction

Isotropic polycrystalline ice, also known as granular ice, is one form of the only stable phase of ice at atmospheric pressure on Earth. Its mechanical behavior has been extensively studied and is now relatively well known under creep and quasi-static conditions [14]. Dynamic loading is of concern in situation of ice impacts on structures. Hailstones or frost for instance can severely damage buildings, aircrafts or trains. An accurate understanding of the ice dynamic response is of interest to provide relevant dimensioning of the structures sollicitated.

The experimental studies conducted so far were focused on the validation and/or the development of new material models for ice impact analysis. In this purpose ice dynamic compressive behavior has been investigated by performing simple compression on Split Hopkinson Pressure Bar ([6], [15], [17]). Authors found a slight positive strain rate sensitivity of the dynamic compressive strength of ice. The

strength values lies from 19 MPa to 58.4 MPa over the range of strain rate employed [60 : 2600 s^{-1}]. It is worth noting that the dispersion in these studies are consequent. Moreover a possible inertial confinement during these tests could be responsible of the strain-rate hardening observed. The dynamic behavior of ice can also be studied by means of experiment of direct ice impact on mechanical structures ([2], [10]). The results obtained from these tests were mostly used to validate numerical modelling of ice ball impact and, then, do not propose any identification of strength values for ice.

All the studies mentioned above took very little care of the ice microstructure resulting from the specific growth processes they used. Depending on the growth procedure, ice microstructure can strongly differs, and either ressemble an ice single crystal or a bubbly ice polycrystal. Both material are expected to have different mechanical response [14]. This lack of consideration about the microstructure is problematic as the microstructural properties are involved in the different damage mecanisms observed at high loading rates in quasi-brittle materials [4]. Regarding tension, to our knowledge, only Lange and Ahrens [7] investigated the dynamic response of ice. In their work, ice specimens were tested in plate impact experiments and a tensile strength of about 17 MPa was measured at a strain rate of 10^4 s^{-1}. There seems to exist no study of the strain rate sensitivity of the ice dynamic tensile strength as the one performed for other brittle materials such as concrete or ceramics ([13], [18]). Though, the tensile strength is at the forefront among all the mechanical parameters that should be investigated and identified in order to get satisfying modelling.

This study aims to fill this gap by providing complementary datas to the first reproductible and robust set of experiments to measure the dynamic tensile strength of polycrystalline ice and to assess its sensibility to the strain rate presented in Saletti et al. [12]. Two different microstructures, with different porosity but similar grain size and shape, are considered in order to investigate the effect of the porosity on the dynamic ice response, the bubbles being expected to act as critical deffects during crack initiation. The studied material and the method used are presented in details in a first section. Then the results are analyzed and discussed before concluding on the strain rate sensitivity at high strain rate and the effect of microstructure.

2 Material and method

2.1 Specimen description

The material studied is artificial polycrystalline ice grown in laboratory. Two microstructures have been designed : a microstructure with a low-air content ($\approx 1-2\%$, named LP for "Low-Porosity" in the following) and a microstructure with a high air content ($\approx 7-10\%$, named HP for "High-Porosity" in the following). Both microstructures are obtained using similar growth technique inspired by the one described in Barnes et al. [1]. Specimens are grown out of isotropic seeds made of crushed ice (with a maximum particle diameter of 2 mm) surrounded by water at 0°C. The slurry is placed on a Peltier element (-15°C), in a 0°C room, to grow gently from bottom to top, and avoid internal stresses during freezing. To obtained the LP microstructure, the isotropic seed is pumped before adding the water. The air trapped between the snow grains is maintained in order to produce the HP microstucture.

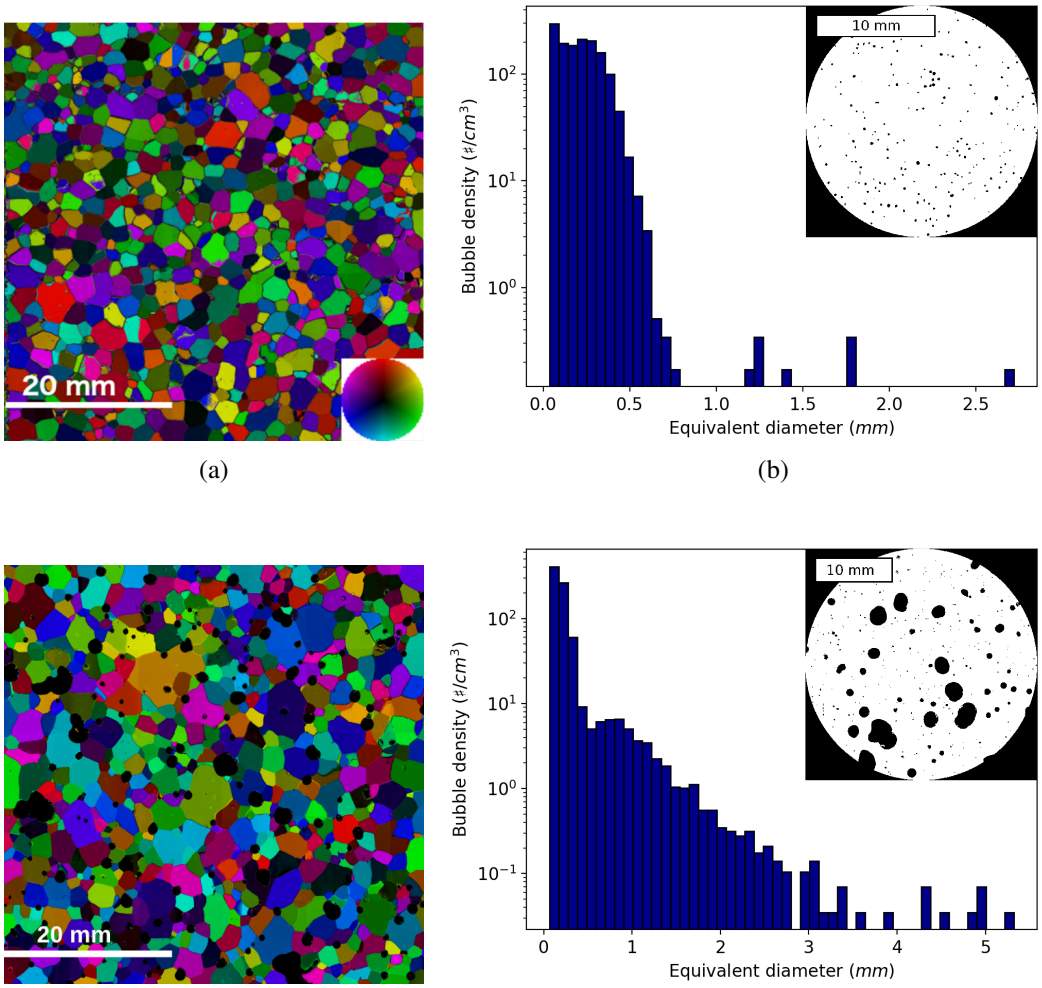

Figure 1: (a) and (c) Microstructure colour-coded with the [0001] crystallographic axis orientation of LP and HP specimens respectively, as measured with an Automatic Ice Texture Analyzer [16]. (b) and (c) Bubble size distribution associated to the LP and HP microstructures respectively. The distributions were extracted from X-Ray tomography scans at a resolution of 14 microns (LP) and 25 microns (HP). A slice view binarized is shown for each microstructure.

Both microstructures have equi-axed grains and an isotropic crystallographic texture, the mean grain size being about 1 to 2 mm (see figure 1(a) and 1(c)). A detailed description of the bubble size distribution is obtained via X-rays tomography analysis. An example is given in figure 1(b) and 1(d) for each microstructure. The main difference between these two distributions is the presence in the HP microtructure of a large amount of bubbles whose the equivalent diameter exceeds $0.8\ mm$ (population A). This feature is not observed in the LP bubble size distribution where only few bubbles are larger than $0.8\ mm$. The distributions are relatively similar below this threshold (population B).

2.2 Spalling test technique and experimental set up

The spalling test on Hopkinson bar is a convenient technique to measure the tensile strength of brittle materials and allows to reach strain rate up to 200 s^{-1}. The principle is the following : a short compressive pulse is generated by the impact of a cylindrical projectile on an incident bar of 45 mm in diameter

and 1200 mm in length. The projectile is 50 mm long and has a spherical-cap-ended nose to act as a pulse shaper in order to smooth the loading pulse [3]. The compressive wave propagates along the bar and the specimen to reach the free surface of the latter. The wave is then reflected as a tensile pulse creating tension inside the specimen. Obviously this method is suitable for materials whose the compressive strength is higher than its tensile strength which is the case for ice, at least in the quasi-static range [11]. The specimen is approximately of the same diameter of the bar and 120 mm long.

The Hopkinson bar is instrumented with a strain gauge to measure the compressive pulse applied to the specimen. A reflective paper is glued at the free-end of the specimen allowing the measurement of the material velocity of this rear face by a laser interferometer (see figure 2). The tests are filmed with an ultra high speed (UHS) camera, the acquisition rate is 1 $Mfps$. A more precise description of the experimental set up can be found in Saletti et al. [12].

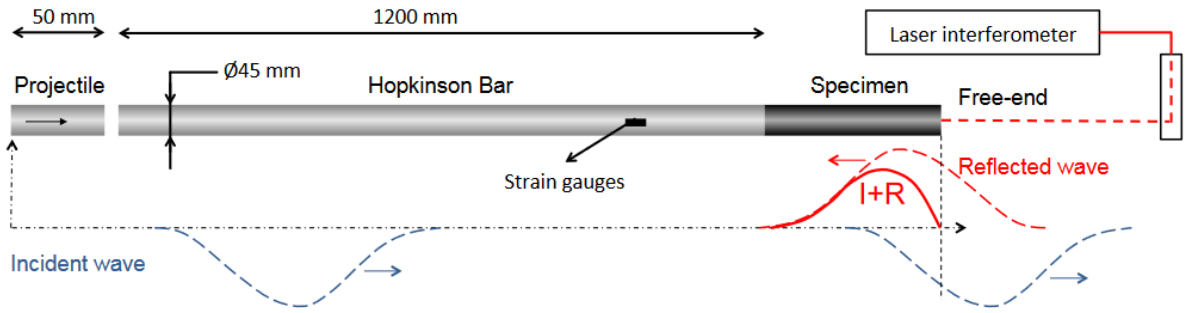

Figure 2: Scheme of the spalling test set-up used in the experiments.

As the major difficulty being the ambient temperature of the spalling room that far exceeds the ice melting temperature, several arangements have been made. The specimens are stored in a deep-freezer set at $-30°C$ near their final position in the experimental set-up. A protocol has been established in order to ensure that less than 30 seconds elapse between the time when the specimen is taken out from the deep-freezer and the time when it is loaded by the spalling test apparatus. A cylinder made of the same aluminium alloy as the one of the input bar is glued on the specimen during its preparation in cold room. This cylinder is 45 mm in diameter and two lengths were used, 30 mm and 40 mm. Its main roles are (i) to avoid a thermal shock between the ice specimen and the Hopkinson bar which is at room temperature; (ii) to delay the melting of the specimen on its bar side face.

2.3 Signal processing

Only the material velocity of the specimen rear face and the strain in the incident bar at the strain gauge location are measured during the test. By determining the time delay Δt between these two points, one can compute the longitudinal acoustic wave velocity $C_{specimen}$ in the specimen (see figure 3). Then by assuming a pure elastic behavior prior to brittle failure, the linear acoustic approximation detailed in Novikov et al. [9] can be used to compute the ultimate spalling strength of the specimen :

$$\sigma_{spall} = \frac{1}{2}\rho_{specimen} C_{specimen} \Delta V \tag{1}$$

where $\rho_{specimen}$ is the density of the specimen. The term ΔV represents the pullback velocity corresponding to the difference between the maximum velocity and the velocity at rebound that are measured on the rear face of the specimen (see figure 3). The elastic modulus is given by :

$$E = \rho_{specimen} C^2_{specimen} \tag{2}$$

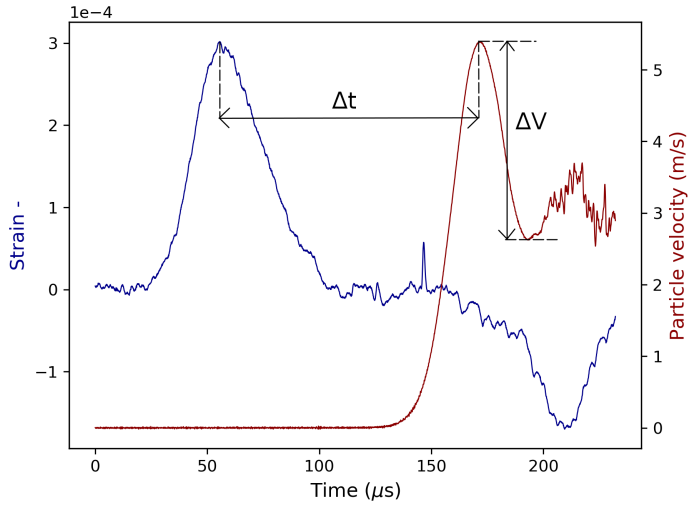

Figure 3: Typical signals recorded during a spalling test by the strain gauge (blue curve) and by the interforemeter laser (red curve).

The strain-rate can not be measured directly as it is too complex to glue strain gauges on the ice surface. An elastic numerical simulation with the software ABAQUS-explicit is required. For each test the velocity profile is artificially converted into an elastic profile. This is achieved by using the rear-face velocity measurement up to the rebound due to spalling. After this point, this curve is virtually prolongated keeping the slope of the tensile phase before spalling fracture occured. The stress corresponding to the material velocity $V(t)$ according to the equation 3 is used as a loading pulse in the numerical simulations.

$$\sigma_T(t - \Delta t) = \frac{1}{2} \rho_{specimen} C_{specimen} V(t) \tag{3}$$

2.4 Test validity

Several indicators are available to assess the quality of each test. As the major risk is the initiation of cracks due to compression loading, the images of the UHS camera are carefully analyzed in order to detect any compressive damage.

Another source of error is the quality of the interface between the aluminium insert and the specimen where the presence of water due to premature melting of the ice is possible. In this case, although the specimen is still undergoing compression and tension, the input stress is not completely transmitted. Two criterions can be considered here, the first one consists in comparing the wave velocity measured to an a priori standard value of ice :

$$C_{ice} = \sqrt{\frac{E_{ice}}{\rho_{ice}(-30C)}} = \sqrt{\frac{9.33\ GPa}{921.6\ kg.m^{-3}}} = 3182\ m/s \tag{4}$$

whith E_{ice} and ρ_{ice}, the elastic modulus and the corrected density (according to the temperature) of the ice polycrystal respectively [5].

For the second criterion the ratio α_{exp} of the transmitted energy into the specimen over the incident energy from the incident bar is compared to a theoretical ratio α_{th} given by :

$$\alpha_{th} = \frac{2}{\frac{Z_{bar}}{Z_{specimen}} + 1} \tag{5}$$

with Z_{bar} and $Z_{specimen}$ the acoustic impedance of the incident bar and of the specimen respectively [8]. If the ratio α_{exp}/α_{th} is close to 1 the interface between the ice and aluminium is supposed to be of good quality.

3 Results and discussion

3.1 Tensile strength results

Several experimental campains have been carried out. 11 test with HP specimens and 9 with LP specimens are finally considered (see figure 4) after the quality checking stage. The strain rates applied range between 24 and 112 s^{-1} and between 41 and 120 s^{-1} for HP and LP specimens respectively. The spalling stresses measured, i.e. tensile strengths, increase from 0.8 to 3.0 MPa and from 1.9 to 5.3 MPa over these ranges for HP and LP specimens respectively.

The results presented in figure 4 highlight a variation of the spalling strength, i.e. tensile strength, with the strain rate applied. Since temperature conditions were repeatable, and since we expect reproductible microstructures in term of grain size and orientations within each sample population (LP and HP), this result evidences a strain-rate sensitivity of the dynamic tensile strength of ice. Unlike to the quasi-static strength that was shown to be of 1 MPa over a large range of strain-rate, i.e. 10^{-7} s^{-1} to 10^{-1} s^{-1} [14]c.

A significant strength weakenning with an increasing porosity is also observable. In brittle materials, the final fragmentation is the result of a competition between the activation of critical defects and the obscuration phenomenom [4]. In the microstructures considered in this study, the critical defects are assimilated to bubbles. Consequently for a similar failure stress, LP and HP specimens are expected to present different crack densities due to different bubble distributions. At the loading rates applied during the spalling tests only the bubbles belonging to the population A (i.e. bubbles larger than 0.8 mm in diameter) are activated in the HP specimens. This is not the case in the LP microstructure as the density of bubbles larger than 0.8 mm is too low to relax efficiently the inner stress. The population B is thus activated, recquiring higher energy to achieve the complete fragmentation observed. This result confirms the role of bubbles as a key parameter controlling the ice fragmentation at high loading rates.

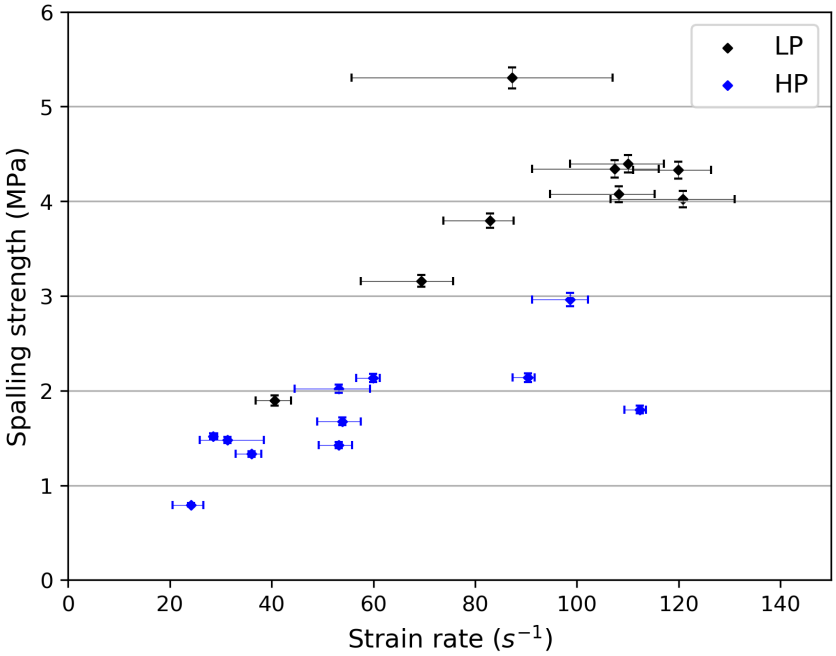

Figure 4: Tensile strength results with strain-rate. The displayed intervals on the curve correspond to the minimum and maximum values of strain rate measured during the tensile phase of the elastic simulations. The markers in between the intervals corresponds to the mean values of determined strain rates

3.2 Image analysis of the fragmentation pattern

The UHS camera allowed to observe the crack propagation in the volume of the specimen during each test. Even if the latter is a qualitative piece of information, it enables to distinguish three main different scenarios as a function of strain rate, at least on the LP specimens where the crack porpagation is more obvious (see figure 5). Test ♯LP15 was one of the test conducted with the lowest value of mean strain rate. In the four pictures presented in Figure 5(a), only one macro crack can be observed. By contrast, at higher strain rates such as in Figure 5(c) (test ♯LP17, 110 s^{-1}), several cracks oriented perpendicularly to the specimen axis develop in a small volume delimited by the white dashed-line rectangle at $T_0 + 66$ μs. In the next steps of the test, this zone of damage spreads out toward the bar side of the specimen as observed on the last image where the light saturates. The cracks can be attributed to tensile loading. Finally, the higher the loading rate, the higher the number of cracks activated, which is consistent with the behaviour expected for brittle materials [4].

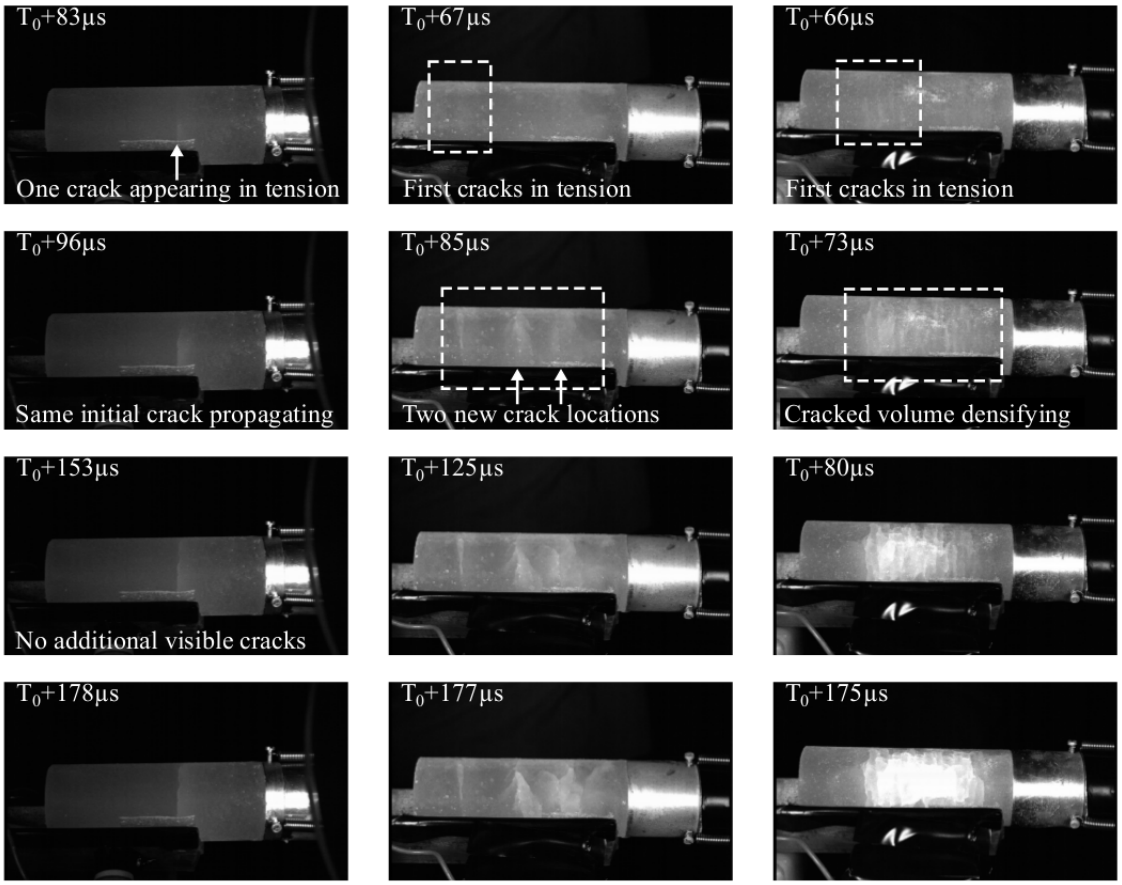

Figure 5: Fracture in the specimen for three different strain rates. Left : LP15 (41 s^{-1}). Middle : LP21 (69 s^{-1}). Right : LP17 (110 s^{-1}). The evolution of the number of cracks clearly visible with the UHS camera increases with the strain rate.

4 Conclusion

This paper presents a complementary study to Saletti et al. [12] by investigating the dynamic tensile behavior of two different microstructures of ice, subjected to strain rate ranging from 24 to 120 s^{-1}. This was achieved by adapting the spalling test technique to the ice material. The experimental procedure is carefully presented and three indicators are proposed to validate each test: a qualitative optical analysis with an ultra-high-speed camera, a quantitative measurement of the wave speed in the material and a quantitative analysis of the quality of the contact with the α ratio. 50 specimens were prepared and 20 tests considered to present the final results based on the Novikov approximation. The results show that tensile strength is clearly influenced by the strain rate and the porosity. The analysis of the fracture patterns occurring in the specimen during the test confirm also the elastic brittle behaviour in tension of ice at this range of strain rates.

Acknowledgements

The present work was developped in the framework of the Brittle's Codex chair (Fondation UGA) and thanks to the support from the CEA-CESTA (France). The provided support and fundings are gratefully ackowledged by the authors.

References

[1] P Barnes, David Tabor, and JCF Walker. The friction and creep of polycrystalline ice. *Proc. R. Soc. Lond. A*, 324(1557):127–155, 1971.

[2] Alain Combescure, Yann Chuzel-Marmot, and Jacky Fabis. Experimental study of high-velocity impact and fracture of ice. *International Journal of Solids and Structures*, 48(20):2779–2790, 2011.

[3] Benjamin Erzar and Pascal Forquin. An experimental method to determine the tensile strength of concrete at high rates of strain. *Experimental Mechanics*, 50(7):941–955, 2010.

[4] Pascal Forquin and François Hild. A probabilistic damage model of the dynamic fragmentation process in brittle materials. In *Advances in applied mechanics*, volume 44, pages 1–72. Elsevier, 2010.

[5] PH Gammon, H Kiefte, MJ Clouter, and WW Denner. Elastic constants of artificial and natural ice samples by brillouin spectroscopy. *Journal of glaciology*, 29(103):433–460, 1983.

[6] Hyonny Kim and John N Keune. Compressive strength of ice at impact strain rates. *Journal of materials science*, 42(8):2802, 2007.

[7] Manfred A Lange and Thomas J Ahrens. The dynamic tensile strength of ice and ice-silicate mixtures. *Journal of Geophysical Research: Solid Earth*, 88(B2):1197–1208, 1983.

[8] Marc A Meyers. *Dynamic behavior of materials*. John wiley & sons, 1994.

[9] S Novikov, D I.I., and I. A.G. The study of fracture of steel, aluminium and copper under explosive loading. *Fizika Metallov i Metallovedenie*, 21:608, 1966.

[10] Jesús Pernas-Sánchez, José Alfonso Artero-Guerrero, D Varas, and Jorge López-Puente. Analysis of ice impact process at high velocity. *Experimental Mechanics*, 55(9):1669–1679, 2015.

[11] JJ Petrovic. Review mechanical properties of ice and snow. *Journal of materials science*, 38(1):1–6, 2003.

[12] D Saletti, D Georges, V Gouy, M Montagnat, and P Forquin. A study of the mechanical response of polycrystalline ice subjected to dynamic tension loading using the spalling test technique. *International Journal of Impact Engineering*, In press.

[13] Harald Schuler, Christoph Mayrhofer, and Klaus Thoma. Spall experiments for the measurement of the tensile strength and fracture energy of concrete at high strain rates. *International Journal of Impact Engineering*, 32(10):1635–1650, 2006.

[14] Erland M Schulson and Paul Duval. *Creep and fracture of ice*. Cambridge University Press, 2009.

[15] Mostafa Shazly, Vikas Prakash, and Bradley A Lerch. High strain-rate behavior of ice under uniaxial compression. *International Journal of Solids and Structures*, 46(6):1499–1515, 2009.

[16] Christopher JL Wilson, David S Russell-Head, and Hadi M Sim. The application of an automated fabric analyzer system to the textural evolution of folded ice layers in shear zones. *Annals of Glaciology*, 37:7–17, 2003.

[17] Xianqian Wu and Vikas Prakash. Dynamic strength of distill water and lake water ice at high strain rates. *International Journal of Impact Engineering*, 76:155–165, 2015.

[18] JL Zinszner, P Forquin, and G Rossiquet. Experimental and numerical analysis of the dynamic fragmentation in a sic ceramic under impact. *International Journal of Impact Engineering*, 76:9–19, 2015.